



OPEN ACCESS

EDITED BY

Fuqiong Huang,
China Earthquake Networks
Center, China

REVIEWED BY

Ameha Atnafu Muluneh,
University of Bremen, Germany
Jiashun Hu,
Southern University of Science and
Technology, China

*CORRESPONDENCE

P.J. Heron,
✉ Philip.heron@utoronto.ca

RECEIVED 23 October 2025
REVISED 30 January 2026
ACCEPTED 17 February 2026
PUBLISHED 12 March 2026

CITATION

Zhong R, Rich JE and Heron PJ (2026)
Earthquake swarms on the Mid-Atlantic
Ridge: assessing the applicability of a
global catalogue for seismic analysis.
Front. Earth Sci. 14:1731117.
doi: 10.3389/feart.2026.1731117

COPYRIGHT

© 2026 Zhong, Rich and Heron. This is
an open-access article distributed
under the terms of the [Creative
Commons Attribution License \(CC BY\)](#).
The use, distribution or reproduction in
other forums is permitted, provided the
original author(s) and the copyright
owner(s) are credited and that the
original publication in this journal is
cited, in accordance with accepted
academic practice. No use, distribution
or reproduction is permitted which
does not comply with these terms.

Earthquake swarms on the Mid-Atlantic Ridge: assessing the applicability of a global catalogue for seismic analysis

R. Zhong¹, J. E. Rich² and P. J. Heron^{1*}

¹Department of Physical and Environmental Sciences, University of Toronto Scarborough, Toronto, ON, Canada, ²Department of Earth Sciences, University of Toronto, Toronto, ON, Canada

The Mid-Atlantic Ridge is mostly positioned at great distances from on-land seismic stations. As a result, analyses of earthquakes are challenging, with focused studies often coming through temporary local recording devices. Although previous work has explored batches of local earthquakes (known as swarms) to uncover information on plate tectonic boundary kinematics, there has been limited large-scale analysis of swarms across the ridge. Here, we take a global earthquake dataset and apply cluster analysis to produce an overview of swarm dynamics across the Mid-Atlantic Ridge latitudes 52°N and 63°N (a portion of Reykjanes Ridge). Our work produces over 150 swarms as compared to only 6 swarms discussed in previous work for the same location and time period. In particular, the swarms generated from this dataset are fleeting in time (<24 h) and stable in location (<20 km). The work here also outlines the limitations of using such a generic global dataset and highlights that this study is unable to fully capture the seismic dynamics of a Mid-Atlantic Ridge earthquake event. However, this methodology of large-scale analysis of a broad dataset can supplement local high-resolution data with quantity of swarm events over quality of seismic characteristics. Here, we provide an overview of timing, location, and occurrence of swarms—identifying potential areas for future exploration.

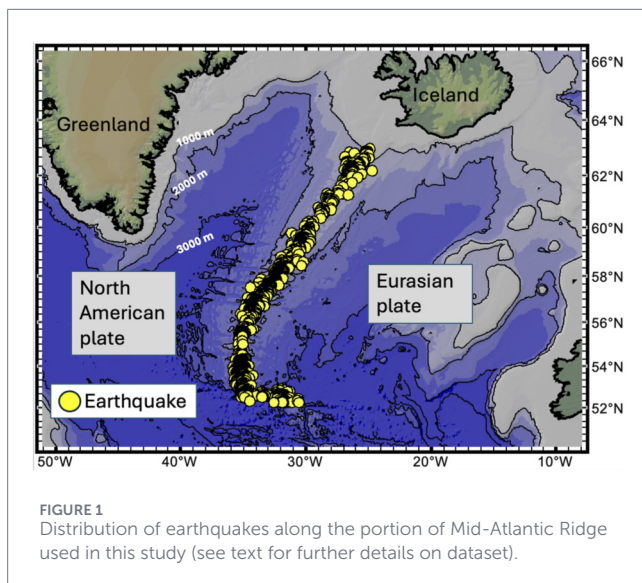
KEYWORDS

cluster analysis, earthquake swarms, global catalogue, Mid-Atlantic ridge, plate tectonics

1 Introduction

The Mid-Atlantic Ridge (MAR) is the longest divergent plate boundary in the world, with evident seafloor spreading (Bergman and Solomon, 1990), transform faults (Wilson, 1965; Schlaphorst et al., 2023), and hydrothermal vents (German et al., 2008) generating earthquakes as the Eurasian and African plates move away from the North and South American plates (e.g., Figure 1). Plate tectonic processes have been linked to the establishment of life on our planet (Cox et al., 2018), yet the slow process of plate divergence and ridge mechanics occur at great distances from land and are therefore inherently hard to examine.

Earthquake swarms, generally defined as a sequence of earthquakes lacking a mainshock event (Björnsson et al., 2020; Läderach et al., 2012; Brocher, 1983; Klein, 1976), can occur across the ridge for a range of tectonic mechanisms (e.g., spreading, magma venting, faulting) (Klein, 1976; Bergman and Solomon, 1990). Specific definitions of what constitutes an earthquake swarm have differed from study to study, using anything



from event rates (Crawford et al., 2013; Läderach et al., 2012) to the number of events in the sequence (Schlindwein, 2012) to spatial and temporal constraints (Bergman and Solomon, 1990).

From the published literature on earthquake swarms or sequences on the MAR, we have identified 151 swarms across the whole ridge (Supplementary Table S1), spanning from 1944 until 2022 (Bergman and Solomon, 1990; Björnsson et al., 2020; Bohnenstiehl et al., 2002; Bohnenstiehl et al., 2003; Brocher, 1983; Crane et al., 1997; Crawford et al., 2013; de Melo et al., 2021; Dziak et al., 2004; German et al., 2008; Giusti et al., 2018; Goslin et al., 2005; Klein, 1976; Smith et al., 2002; Cesca et al., 2023). Although several papers have collated data to identify individual swarms on the ridge (e.g., 34 swarms analysed by Bergman and Solomon, 1990), there still lacks a comprehensive database for swarms across the Mid-Atlantic Ridge due to the pervasive challenge of consistent data acquisition locally to the ridge. As a result, *in-situ* studies often implement a range of techniques for capture over a short time period. However, the diversity of data collection methods when analysing different swarms (e.g., hydrophone, deep-tow sidescan sonar, local seismometers) makes it difficult to produce even a basic comparison between swarms in the same region.

In this study, we analyse a global earthquake dataset that can compare swarms within the same region equally, rather than relying on multiple instances of short-term data employment. We use this method to explore any similarities in spatial, temporal, and quantity characteristics between swarm events. Given the difficulty in capturing low magnitude earthquake activity, we also provide an assessment of the applicability of this method to understand basic seismic characteristics. As previous work on swarms of the Mid-Atlantic has focused on individual groups of seismicity (e.g., de Melo et al., 2021; Dziak et al., 2004; German et al., 2008; Giusti et al., 2018; Goslin et al., 2005), this study takes a step towards larger data analysis of swarm characteristics.

In the following sections, we outline our criteria for choosing a portion of the ridge to analyse with the global database (Section: Database), then describe our method of swarm classification

(Section: Method) and subsequent Results. The work here finishes with a Discussion that features a comparison with our results and previously studied events, as well as an assessment of the applicability of the work.

2 Database and choice of study area

For our earthquake data, we use the available United States Geological Survey (USGS) earthquake database (U.S. Geological Survey, 2024a) as our global catalogue to analyse earthquake events across a section of the MAR over the past 25 years (Figure 1). Data was downloaded from the USGS Earthquake Catalog (U.S. Geological Survey, 2024b) with search parameters of time (2000-01-01 00:00:00 to 2024-09-01 00:00:00) and type (earthquake). This data was then filtered by distance from the Mid-Atlantic Ridge (MAR) using vector data (Hasterok et al., 2022), removing any earthquakes more than 50 km from the MAR on either side.

As the work here is to assess if there is any simple swarm classification of Mid-Atlantic Ridge activity that can be made from a global dataset, we have only used a small portion of the ridge to produce the best opportunity for ‘quality’ earthquakes (e.g., earthquakes similar in tectonic mechanism and of similar magnitude). First, we divided the ridge into different portions and systematically tested for quality.

Our global database was subsequently divided into 4 sections of relatively similar earthquake events (Figure 2): Reykjanes Ridge (52.27°N to 63°N), Northern MAR (15°N to 52.27°N), Central MAR (2°S to 15°N), and Southern MAR (55°S to 2°S). The divisions between each section were chosen based on the shape of the MAR, with relatively straight portions of the MAR in each section. These definitions were compared with USGS definitions of place as part of the database for consistency (U.S. Geological Survey, 2024b). Table 1 shows the ranges of the sections, number of earthquakes in the regions and the magnitude information (also shown in Figure 2). Despite contrasting section lengths (Figures 2a–e), the sections have a similar number of earthquakes (between 1,600 and 2,000 over 25 years) (Table 1). We did not analyse earthquakes in a complex volcanic region such as within the proximity of the Icelandic plume (e.g., latitudes larger than 63°N) in an attempt to keep a similar tectonic environment between the events.

A test for quality of data and consistency of earthquake mechanism was to analyse earthquake magnitude in the different sections (Figure 2f). As mentioned, there is difficulty in capturing smaller magnitude earthquakes across the ridge due to the reliance of the USGS global earthquake catalog on teleseismic events (e.g., Bergman and Solomon, 1990). The variability in the earthquake magnitudes captured across the different sections of the MAR shows an uneven data quality across the ridge. In this test, Reykjanes Ridge performs better than the other regions, showing the widest range of magnitudes captured, the lowest average magnitude, and the joint lowest recorded magnitude (Table 1; Figure 2f). As a result, we chose to explore swarms of the Reykjanes Ridge only (latitudes 52.27°N to 63.00°N), given the variable data quality in other regions.

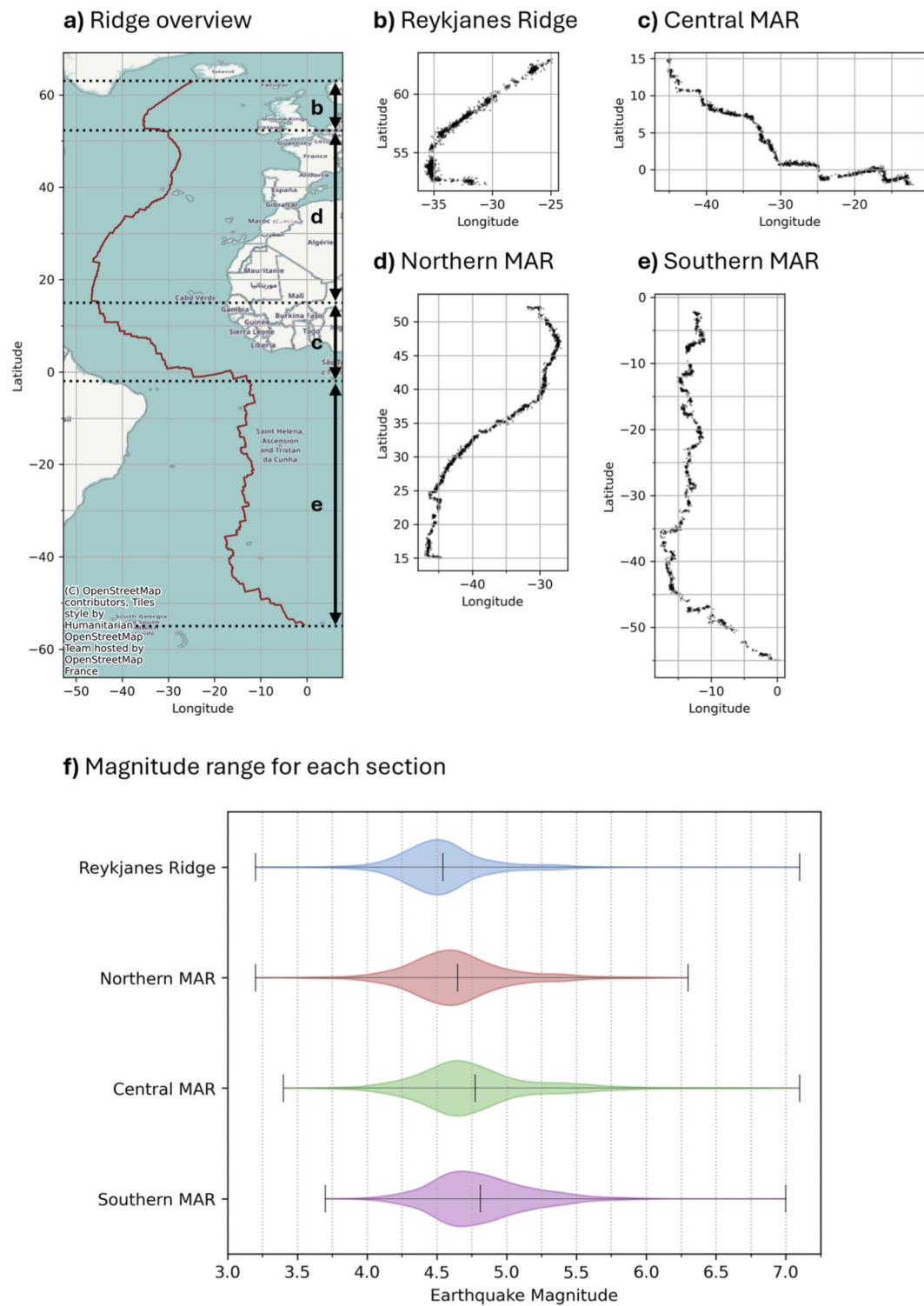


FIGURE 2 Distribution and range of earthquake magnitudes for the different Mid-Atlantic Ridge sections. **(a)** Map of the different sections of the Mid-Atlantic Ridge (MAR) delineated by dotted lines going from north to south: Reykjanes Ridge; Northern MAR; Central MAR; Southern MAR. Locations of earthquakes from the database are plotted as dots on latitude and longitude maps for **(b)** Reykjanes Ridge; **(c)** Central MAR; **(d)** Northern MAR; and **(e)** Southern MAR. **(f)** Violin plots showing earthquake magnitudes for all the data (see [Table 1](#)).

TABLE 1 Overall data statistics for the Mid-Atlantic Ridge. This table excludes magnitude values of 0.0 (1.9% of entire dataset) for the average, lowest, and highest magnitude columns. Data range from 2000 to 2024 (see Method for more details). Latitude range shows lower latitude bound (inclusive) and upper latitude bound (exclusive).

Section name	Latitude range	Number of earthquakes	Average magnitude	Lowest magnitude	Highest magnitude
Reykjanes Ridge	[52.27, 63.00)	1,703	4.54	3.2	7.1
Northern MAR	[15.00, 52.27)	1,997	4.65	3.2	6.3
Central MAR	[-2.00, 15.00)	1,636	4.78	3.4	7.1
Southern MAR	[-55.00, -2.00)	1,702	4.81	3.7	7.0
Total	[-55.00, 63.00]	7,038	4.69	3.2	7.1

Bold text in final row shows the total values for each column

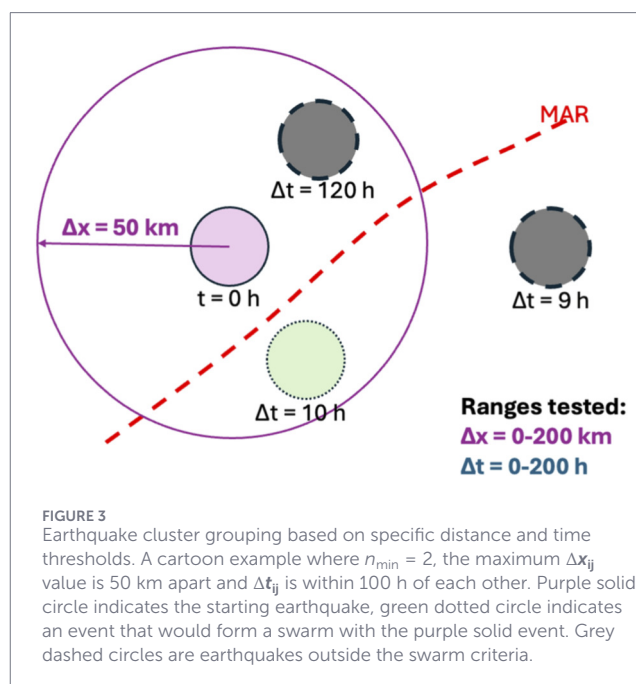
3 Methods

For this study, we apply a simple cluster analysis to identify basic swarm characteristics for a portion of the Mid-Atlantic Ridge. In the previous section, we identified the Reykjanes Ridge between 52°N and 63°N as a portion of the MAR that may be suitable for swarm assessment and analysis. To capture swarms, we developed a Python module (Zhong et al., 2026) to take a table of earthquakes as an input and produce a table of swarms as its output. For the cluster analysis, three parameters need to be specified:

- minimum number of earthquakes that constitutes a swarm (n_{min});
- upper threshold for distance Δx_{ij} , where j is a given earthquake, i is spatially the closest preceding earthquake in a given swarm, and Δx_{ij} is the distance between earthquakes i and j (Δx); and
- upper threshold for Δt_{ij} , where j is a given earthquake, i is temporally the closest preceding earthquake in a given swarm, and Δt_{ij} is the difference between the time of occurrence for earthquakes i and j (Δt).

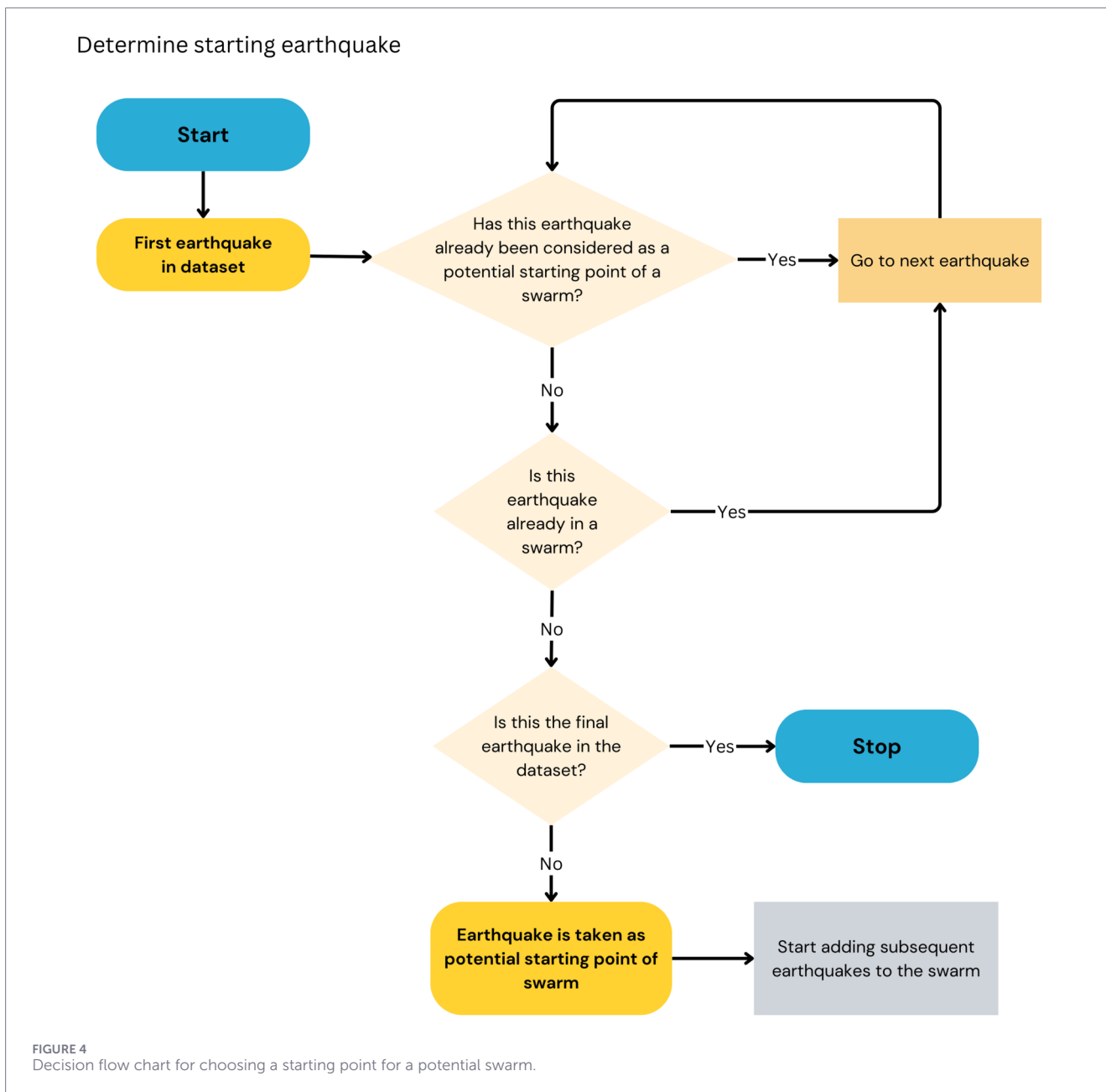
The minimum number of earthquakes here has been set to 2, as that is the smallest swarm possible. The earthquake input data is ordered chronologically, then the first earthquake is taken as the starting point of a potential swarm. An earthquake is added to a swarm if it falls within the maximum delta time and distance specified (Figure 3). That is, the time difference between the current earthquake and the previous earthquake in a swarm must be within the specified time value, and the distance between the current earthquake and at least one previous earthquake in a swarm must be within the specified distance value.

When the current earthquake satisfies both requirements, it is added to the swarm. Earthquakes already in a swarm are not considered for subsequent swarms, so each earthquake can only belong to one swarm. Figures 4, 5 show the flow chart for our classification of earthquakes within a swarm. As we are using a global catalogue and are assessing this database for basic seismic analysis, we only capture the following swarm properties: Start time; End time; Duration; Origin latitude; Origin longitude; Number of earthquakes; and Magnitudes. However, despite the simple nature of the output, the information generated should be of similar quality across the swarms captured (and therefore robust enough for comparison).



In our methodology, we do not exclude swarms based on the magnitude. In this analysis we assume that all events in this region are swarms (where the magnitude of all events in a swarm are similar) rather than filter for any mainshock-aftershock events (where there is a larger magnitude main event followed by smaller magnitude earthquakes). We do this to avoid setting strict criteria for what constitutes a swarm, given that there is not a firm definition of this scenario. We analyse the impact of this methodology choice in our Discussion section.

Our Python module was then applied to the data for different criteria of distance (Δx) and time (Δt). Specifically, we tested 400 different combinations of time and distance values ranging from 10 to 200 h and 10–200 km (i.e. 10 h and 10 km, 10 h and 20 km, ..., 10 h and 200 km, 20 h and 10 km, ..., 200 h and 200 km). The number of swarms in the output were evaluated for each combination, based on the criteria of Δx and Δt , and are described in the following Results section.



4 Results

4.1 Different combinations of Δx and Δt

Figure 6a shows the number of swarms captured for each of the 400 combinations of Δt (x-axis) and Δx (y-axis) thresholds applied to the earthquake data of this section of the MAR (52°N to 63°N, Figure 2b). Despite the range of Δx and Δt thresholds spanning 200 km and 200 h (respectively), there is low variability in the number of swarms captured (e.g., between 160 and 200 swarms).

Figure 6a shows that the highest number of swarms is captured when the time threshold is the shortest (10 h) and the distance threshold is the longest (200 km). However, increasing the time threshold and keeping the distance threshold at 200 km reduces the number of swarms captured (as shown by the change in colour

along the top row of Figure 6a). This is due to the amalgamation of smaller clusters into one larger cluster as the time threshold increases.

However, there is limited change in the number of swarms being captured as the time or distance thresholds are increased. Figure 6b displays the percentage change of when increasing the distance threshold (Δx). For instance, the bottom-left data point of Figure 6b (open green arrow) describes the increase in swarms captured when applying $\Delta t = 10$ h but increasing from $\Delta x = 10$ km to 20 km. The highest percentage increase of swarms (around 10%) occurs when applying $\Delta t = 30$ h but increasing from $\Delta x = 10$ km to 20 km (solid blue arrow).

After increasing to 50 km distance, the percentage change in number of swarms captured is limited, with the values falling between -5% and +5% (dashed line, Figure 6b). This indicates that

Adding subsequent earthquakes to a swarm

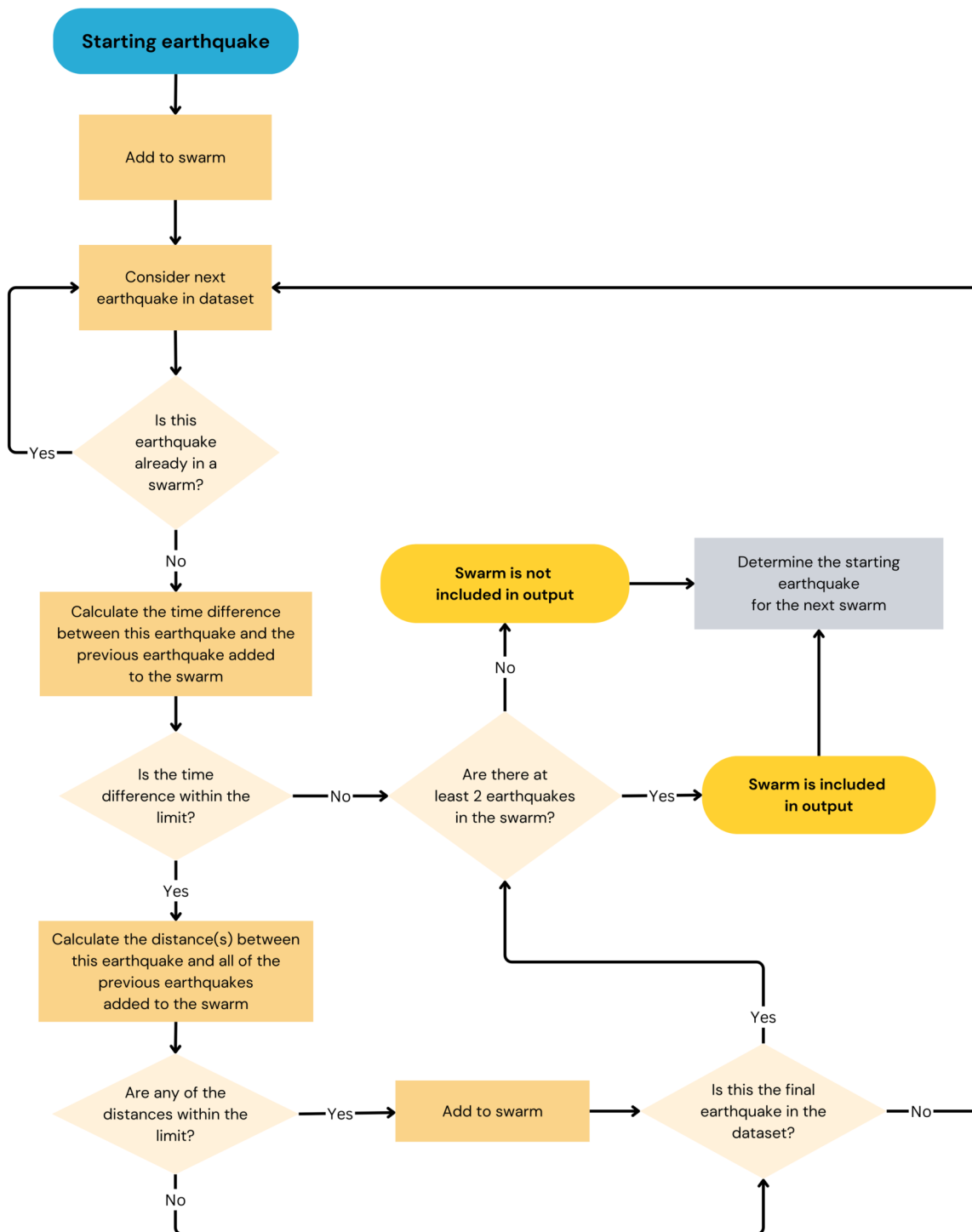


FIGURE 5 Decision flow chart for determining if a subsequent earthquake may be part of a swarm.

once the 50 km distance threshold is reached, there is limited change in the swarms captured. Specifically, the difference in the number of swarms collected with a 50 km threshold at a short period of 10 h and a long period of 100 h is only 17 swarms (8% change).

As a result of this discovery of swarm characteristics within our data, we fix the distance threshold at 50 km for the remainder of the study (and explore the impact of changing the time threshold for swarm capture in the next section).

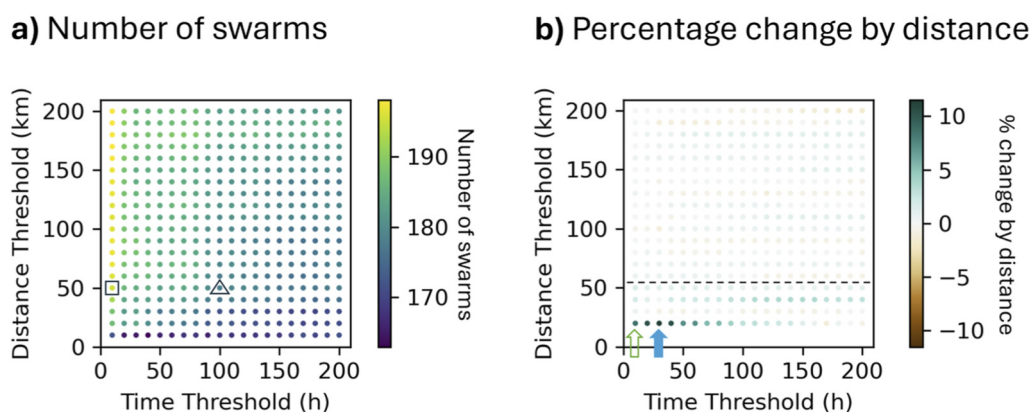


FIGURE 6 Variance in number of swarms captured through simple cluster analysis. **(a)** Number of swarms captured for each combination of time Δt (x-axis) and distance Δx (y-axis) thresholds applied to the earthquake data of a section of the MAR (52°N to 63°N, Figure 2b). **(b)** Percentage change difference when comparing swarms captured for a lower distance threshold. The change in panel b is the difference between the captured swarms and the data point below (e.g., the green open arrow shows the % change in swarms captured between combination 10 h and 10 km with 10 h and 20 km). Solid blue arrow indicates the highest percentage change across the 400 different combinations. Dashed black line highlights that above 50 km distance there is limited change in number of swarms captured. Triangle in panel a highlights the 100 h and 50 km combination, while square indicates 10 h and 50 km combination.

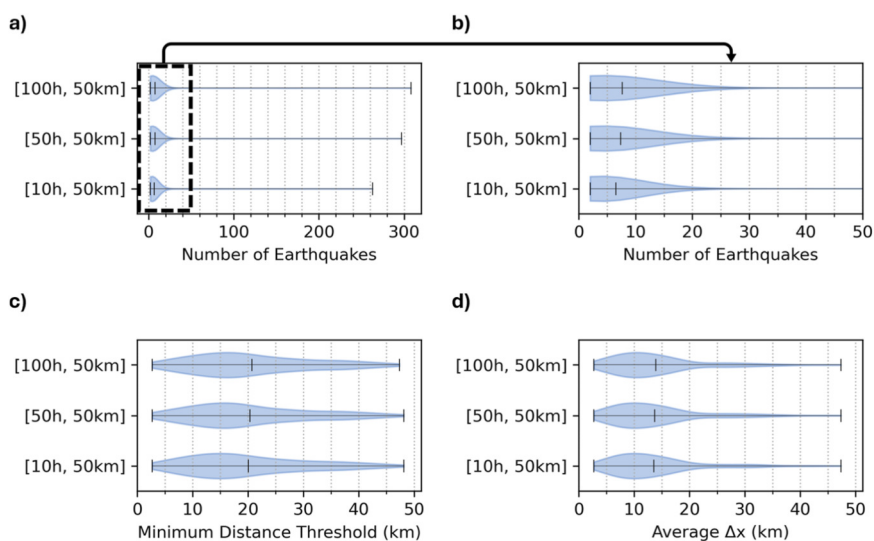


FIGURE 7 Characteristics of earthquake swarms for three different spatial and temporal thresholds ([100 h, 50 km], [50 h, 50 km], [10 h, 50 km]). **(a)** Violin plot of the number of earthquakes within a swarm, with **(b)** zoomed in to see the mean swarm count. **(c)** Violin plot showing the lowest distance threshold (Δx) required to capture a swarm. **(d)** Violin plot showing the average distance between events within a swarm (Δx). Dash on all plots indicates average values.

4.2 Comparison between time threshold combinations

In Figure 7 and Table 2 we produce a comparison between some of the key statistics of the swarms captured. Specifically, we present three different time capture combinations (10 h, 50 h, and 100 h) to show the differences between a short, medium, and long period combination (with distance threshold fixed at 50 km).

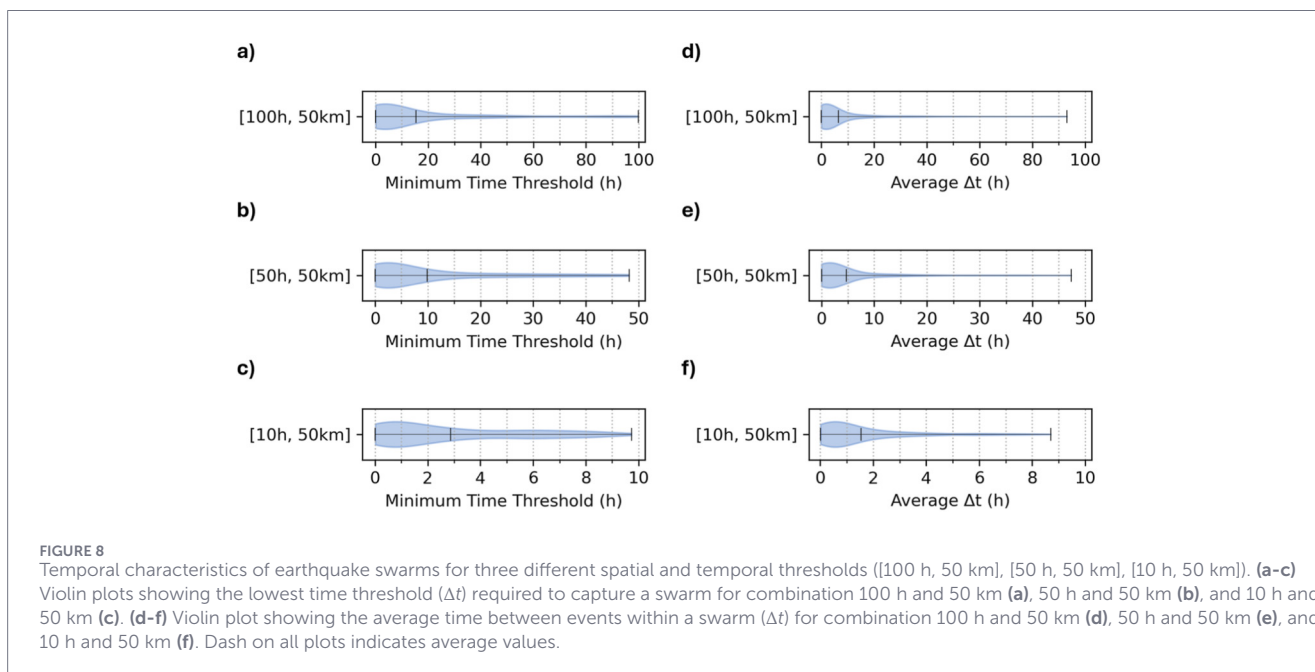
Figures 7a,b (and Table 2) show the number of earthquakes in a swarm given the threshold criteria of 50 km and either 10, 50, or

100 h. This portion of Reykjanes Ridge has an average of 7.7 events per swarm for the 100 h time threshold and 6.5 events per swarm for the 10 h time threshold (Table 2). Therefore, changing the time threshold has a limited impact on the number of events within a swarm from this global catalogue (e.g., a difference of 1.2 events per swarm for 100 h–10 h time threshold).

In Figure 7c, we present the minimum distance threshold required to capture a swarm for the three different combinations. Despite having different temporal components, the spread of the swarms in the violin plot are almost identical, with an average

TABLE 2 Swarm characteristics for different spatial and temporal thresholds. *n* classified as number of swarms, *pop* refers to number of earthquakes in swarm (population), *eq* refers to earthquakes, Δx refers to the distance between events within a swarm, Δt refers to the time between events within a swarm.

Combination	<i>n</i>	Ave pop (eq)	Ave Δx (km)	Ave duration (h)	Ave Δt (h)	% eq in swarm	Max pop (eq)
[100 h, 50 km]	178	7.7	13.9	26	6.5	80%	308
[50 h, 50 km]	183	7.4	13.7	17	4.7	79%	297
[10 h, 50 km]	195	6.5	13.5	6	1.5	75%	263



minimum distance for the swarms of around 20 km. This value indicates that on average a swarm could be captured with only earthquakes falling within 20 km of each other. Figure 7c also shows the minimum distance required for any of the combinations does not fully reach the limit of 50 km (with the 100 h combinations having a value of 47 km as a maximum minimum distance required).

Figure 7d shows the average distance between all the events in the swarm (rather than the minimum distance to capture a full swarm as shown in Figure 7c). The average distance is again similar across the combinations (around 13 km, Table 2), highlighting that on average the swarms captured by this method using this global dataset have earthquakes relatively close to each other (e.g., < 15 km apart, Figure 7d).

Figure 8 outlines the minimum time threshold per swarm (Figures 8a–c) and the average time between events within a swarm (Figures 8d–f) for three different combinations. Figure 8 highlights that the majority of time between events occurs within a day (<24 h). On average, the minimum time threshold required to capture swarm is around 17 h for the long duration combination (100 h, 50 km), which reduces to around 3 h for the short duration combination (10 h, 50 km). Furthermore, the average time between events is around 6.5 h for our long duration combination (Figure 8d) and approximately 90 min for the short duration (Figure 8f).

Table 2 shows the average duration of a swarm (from start to finish) for our short, medium and long duration combinations, with a range of 26 h for our long duration combination and only 6 h for our short-term combination. Table 2 also highlights that of the 1703 earthquakes analysed for this portion of the MAR (Table 1), between 75% and 80% are classified as being in a swarm based on our spatial and temporal combinations.

5 Discussion

The cluster analysis applied here was used to assess whether any swarm signature can be found from a global database of earthquakes on a portion of the Mid-Atlantic Ridge (MAR). Below we'll outline the seismic signatures in the swarms captured from our analysis of 400 different combinations of time and distance thresholds between earthquakes (Figure 6). We'll then outline the usefulness of this method of swarm classification using our global dataset.

5.1 Defining the standard earthquake swarm characteristics for the MAR region

The work here shows that the number of swarms captured is only weakly connected to distance between events. Specifically,

the 400 different combinations of spatial and temporal thresholds shows that a distance threshold of 50 km does not significantly impact the number of swarms captured (e.g., dashed line, Figure 6b). Table 2 provides a summary of three different combinations of spatial and temporal data and highlights that the average distance between events is around 13 km, with Figure 7c showing that a 20 km distance between events would capture most of the swarms. Therefore, from this data, swarms of this portion of the MAR occur within 20 km of each other.

The temporal characteristics of the swarms captured in this study show more variability when changing the threshold for time between events (Figure 6a; Table 2; Figure 8). Overall, increasing the temporal threshold reduces the number of swarms rather than increasing, as shown by a decrease of 17 swarms from applying 10 h threshold to 100 h threshold for a distance of 50 km (Table 2). This change in pattern behaviour could be perceived as being counter intuitive as an increase in threshold should allow for more unique two earthquake events to be captured. Yet, this expectation is not met despite the rather generous definition of what constitutes a swarm (e.g., 2 earthquakes). In this case, by increasing the temporal threshold a small number of swarms combine and become a larger entity rather than several smaller event swarms. However, this impact is slight, given that the average number of earthquakes in a swarm is similar between the longer and shorter combinations (e.g., around 7 events per swarm, Table 2).

Given that the change between both the number of swarms in total and the number of events within a swarm is small when changing the temporal threshold (Table 2; Figure 8), our cluster analysis highlights that time between earthquakes can be fleeting in time. Specifically, if we look at the shortest combination of 10 h between events (at a max distance of 50 km), time between earthquakes can occur within hours (Figures 8c,f) and the total swarm duration is on average 6 h (Table 2).

Based on these findings, in Figure 9a we show our average swarm calculated from our cluster analysis (e.g., Table 2). We show a swarm that has 7 events within it, and an average time and distance between events of 4 h and 11 km, respectively. In Figure 9b we show the largest swarm captured by this method, a 308 earthquake event occurring in September 2022. The importance of highlighting both the average event (Figure 9a) and the largest event (Figure 9b) is that historically only large events are discussed in the literature on MAR swarms (e.g., Goslin et al., 2005; Giusti et al., 2018). Indeed, the event in Figure 9b has been discussed in Cesca et al. (2023), whereas the average event of Figure 9a has not previously been mentioned in academic literature.

Previous work on swarms in the Mid-Atlantic has often focused on a singular event or a short time period in a particular region. Here in this study, we collate and categorize swarms using a generic database to identify potential seismic properties of divergent plate boundary swarms. However, it is important to discuss how our large-scale analysis compares to existing individual studies of swarm dynamics.

5.2 Comparison with published work

In Table 3, we compare our work with five swarms from previous studies (Goslin et al., 2005; Cesca et al., 2023). For the Reykjanes Ridge, we compare our swarm classification (using the liberal 100 h

and 50 km definition) with four swarms from Goslin et al. (2005) and the largest event outlined in Figure 9b (e.g., Cesca et al., 2023).

In Table 3 we show that the method we apply here works well for capturing the latitude and longitude positions and the start time and date of the swarms (in particular for the swarms 1-3). However, in these published papers, the end date of the swarm events are not explicitly mentioned—highlighting a positive of our method as we can establish a defined end date for a swarm through a standardized output for swarm classification. Furthermore, the fourth swarm shows a difference in start time and latitude and longitude, indicating that our method identified an earthquake prior to the published start time of the swarm which could suggest new information surrounding ridge behavior.

However, the number of earthquakes within the swarm are not similar to any of swarms 1-4 – our method consistently underrepresents the number of earthquakes within these published events. The earthquakes documented by Goslin et al. (2005) were recorded by two hydrophone networks moored north and south of the Azores. During its period of operation (05/2002–09/2003), the northern 'SIRENA' network, deployed between latitudes 40° 20'N and 50° 30'N, recorded acoustic signals generated by 809 earthquakes. As a result, it is clear that *in-situ* studies (such as Goslin et al., 2005) highlight that smaller magnitude earthquakes may be naturally excluded from our database method (Figure 2) due to our database's reliance on teleseismic events (e.g., Bergman and Solomon, 1990).

Our largest swarm captured by the data featured 308 events on Reykjanes Ridge, as shown in Figure 9b and outlined in swarm 5 in Table 3. When comparing our swarm 5 with the published literature (Cesca et al., 2023), our work captures a different number of events, latitude start location, and end date. However, these differences can be explained due to the catalogue of Cesca et al. (2023) being more selective, focusing on available hypocentres and moment tensors (and as a result likely removed earthquakes which we have kept).

A 308-event swarm is a clear anomaly in our database (e.g., Figure 7a). Similarly, Cesca et al. (2023) described the swarm as a 'rare example of an energetic, magmatic driven swarm'. As a result, the published literature corroborates our finding of this event being an anomaly for the Mid-Atlantic Ridge and adds to the robustness of our study.

5.3 Method uncertainty

As mentioned, the work here does not incorporate any other dataset than the publicly available USGS data (U.S. Geological Survey, 2024a) and as a result may differ from interpretations based on other existing databases (e.g., Goslin et al., 2005; German et al., 2008; Giusti et al., 2018; de Melo et al., 2021). The USGS database incorporates information about earthquakes from various sources, but it is not a focused, local database for the Mid-Atlantic Ridge region. In particular, the USGS database may be missing several smaller earthquakes from the region given the distance away from the ridge and most on-land recording devices (e.g., smaller events are not strong enough to be captured). As a result, the method presented here does not accurately capture the number of events in a swarm (e.g., Table 3) as compared to *in-situ* studies (e.g., Goslin et al., 2005).

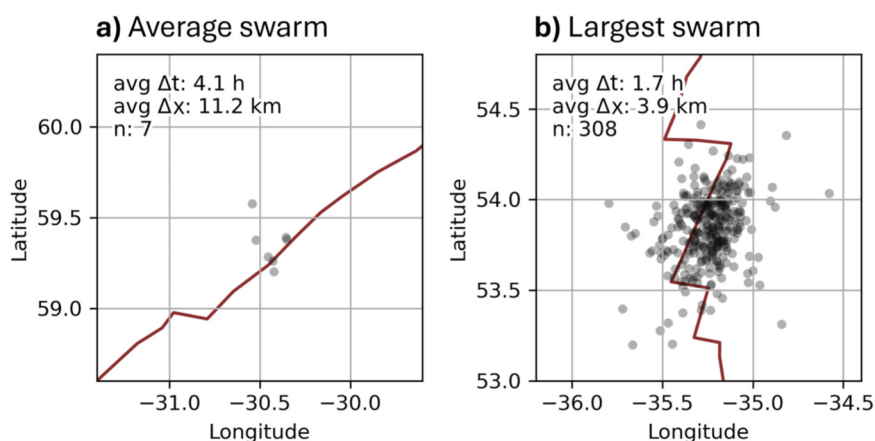


FIGURE 9 Maps of the average swarm characteristics for the Mid-Atlantic Ridge and the largest swarm captured. **(a)** A typical swarm for the Reykjanes Ridge, characterized by a 7-earthquake swarm with an average Δt of 4 h and Δx of 11.2 km (starting at 2004-01-12). **(b)** A map of the largest swarm captured by the method, starting at 2022-09-26. Swarms here generated with the 100 h and 50 km thresholds (Table 2).

TABLE 3 A comparison between the large-scale identification of swarms with previous published Mid-Atlantic Ridge swarms. *Lat* refers to latitude and *lon* refers to longitude, *n* refers to the number of earthquakes within the swarm.

Swarm # and study	n	Lat (°)	Lon (°)	Start date	End date
1 Goslin et al. (2005)	31	59.6	-30.2	2003-01-27	Not defined
1 This study	3	59.5	-30.3	2003-01-27	2003-01-27
1 difference	-28	0.1	0.1	Same	N/A
2 Goslin et al. (2005)	257	57.3	-33.1	2003-02-01	Not defined
2 This study	12	57.2	-33.3	2003-02-01	2003-02-02
2 difference	-245	0.1	0.2	Same	N/A
3 Goslin et al. (2005)	182	58.1	-32.0	2003-07-09	Not defined
3 This study	11	58.1	-32.1	2003-07-09	2003-07-13
3 difference	-171	Same	0.1	Same	N/A
4 Goslin et al. (2005)	35	60.9	-26.9	2003-07-19	Not defined
4 This study	13	61.9	-27.0	2003-07-18	2003-07-20
4 difference	-22	1.0	0.1	1 day	N/A
5 Cesca et al. (2023)	174	53.8	-35.3	2022-09-26	2022-12-10
5 This study	308	54.1	-35.2	2022-09-26	2022-10-18
5 difference	+134	0.3	0.1	Same	Months

Bold text highlights the difference between previous work and this study for the specific swarm.

To explore this further, Figure 10 shows the variability of our swarm data as a function of latitude to test if there are any ridge locations that present a potential drop in reliability. We do this by showing the variability in number of events in a swarm as a function of latitude (Figures 10a,b), as well as the average swarm magnitude (Figure 10c) and average time between earthquakes (Figure 10d).

For context of this reliability test, we outline some potential scenarios that would show data uncertainty. If the swarm data was showing strong variability across the portion of the ridge, it could manifest as a difference in seismic attributes as a function of latitude in the different panels of Figure 10. For example, in

terms of the number of events in a swarm, we may see smaller number of events (e.g., only swarms with 2 events) at particular latitudes. However, Figures 10a,b shows similar ranges of number of events in a swarm across this portion of the ridge. Three instances of high number of events in a swarm (e.g., > 20 earthquakes in a swarm) occur at different latitudes on the MAR, which shows the potential for capturing larger events across the ridge.

Figure 10c shows a potential area for uncertainty in the average swarm magnitude as a function of latitude. For the higher latitudes (>60°N) there is a narrow range of average swarm magnitude (e.g., between 4.1 and 4.7 M), where the rest of the ridge captures lower

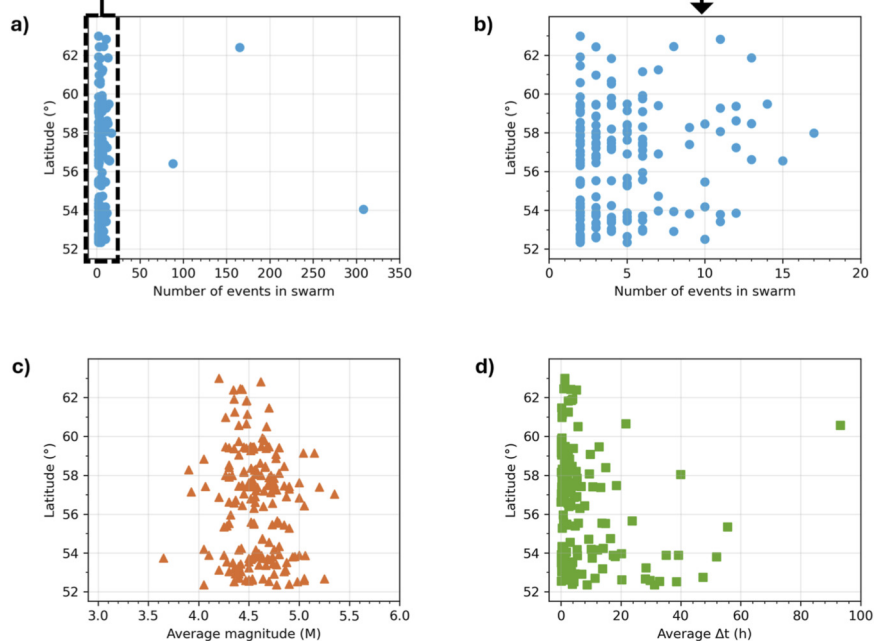


FIGURE 10

Checking the variability of the swarm data as a function of latitude. Plot shows the variability of number of events in a swarm (a–b), average magnitude in a swarm (c), and average time between earthquakes (d). Information presented using the temporal and spatial combination of 100 h and 50 km, respectively.

average magnitudes. This may indicate that either this portion of the ridge is poorly resolved and does not capture lower magnitude events, or that this portion of the ridge behaves differently to the rest of the region (generating earthquakes within a narrow magnitude range). Latitudes below 60°N here exhibit similar average magnitude ranges, which may indicate a more consistent data quality. Figure 10d shows the average time between events as a function of latitude and highlights a number of swarms with an average time of larger than 20 h, particularly between 52°N and 54°N . As a result of this collection of long time period swarms, this region may be another area of potential future exploration for different tectonic mechanisms.

Our cluster analysis here focused on spatial and temporal signatures, rather than other seismic attributes such as focal mechanism and earthquake depth. Given the difficulty in assigning accurate focal mechanism and depths for earthquakes captured at a distance from the ridge (e.g., our global database), we do not analyse these seismic attributes. Instead, we only focus on spatial and temporal signatures. However, there are likely uncertainties related to the location of earthquakes from such a global database—the earthquake locations calculated at a distance from the event are difficult to capture given the magnitude of the events. Yet, Table 3 does show good agreement with the small number of published location of earthquakes, which can act as a marker of accuracy for our dataset.

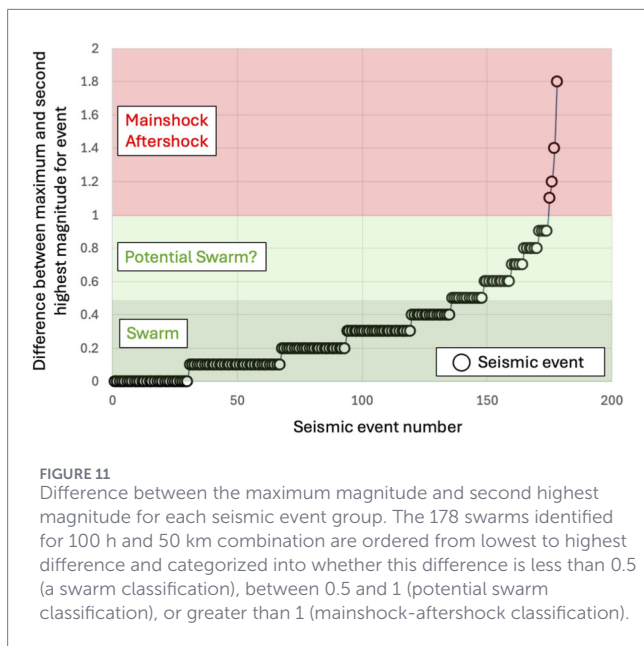
5.4 Swarm or mainshock-aftershock?

As outlined in the Method section, in this study we do not make a specific classification that earthquakes in a swarm must be of similar

magnitude as we wanted to not impose any restrictions or biases on our data analysis. As a result, we may capture some events more similar to a mainshock-aftershock sequence than a swarm events. To address this, in Figure 11 we present the difference between the maximum magnitude event in a swarm and the second highest magnitude of the swarm (for spatial and temporal combination of 50 km and 100 h, respectively). We apply a scaling from McNutt (1996) that offers a general rule of thumb that classifies a mainshock-aftershock sequence if the difference between the highest and second highest magnitude is > 1.0 and classifies a swarm if this difference is < 0.5 (e.g., Läderach et al., 2012).

In Figure 11, the swarms are presented in order of lowest to highest difference between the maximum and second highest magnitude and placed into categories of ‘swarm’ (if difference is 0.5 or below), ‘potential swarm’ (if difference is between 0.5 and 1), and ‘mainshock-aftershock’ (if difference is greater than 1). The spatial and temporal combination of 50 km and 100 h produces 178 clusters in this region of the MAR, with Figure 11 showing that 174 (98%) have a difference between the maximum magnitude and second highest magnitude that is less than 1.

Although our method misidentifies a small proportion of mainshock-aftershock sequences as swarms, the classification of a mainshock-aftershock is quite rigid. Figure 11 shows there is a clear outlier to the rest of the events, which is a mainshock-aftershock event that has a magnitude difference of 1.8. In this anomaly, there was a magnitude 7.1 earthquake (13th February 2015, 52.6°N , 31.9°W) with 9 other earthquakes that produced an average magnitude of 5.0 and a second highest earthquake magnitude of 5.3. Even though this is a clear misidentification



of a swarm, 98% of the remaining events could be well categorized.

5.5 Future work

Future work on this region should focus on understanding the accuracy of the spatial and temporal attributes of the global database. Further comparison between published swarms captured locally to the events would be beneficial to understand the robustness of our simple method presented in this study.

In our work outlined here, we do not apply an area analysis to the swarms we identify—additional work could quantify the convex hull area of the swarms to identify any patterns across the ridge. Furthermore, future work understanding the swarm movement up or down the ridge could prove beneficial in further understanding the kinematics of divergent plate boundaries (Neves et al., 2004).

Potential future application of our work here could be to other sections of the MAR to see if there are any similarities or differences (e.g., Figure 2). As mentioned in the previous section, we only use one global dataset for our analysis. Incorporating a number of different global datasets (e.g., European, Canadian, and African datasets) may add to the discussion on how robust our findings are. This additional amalgamation of databases may allow for a further analysis into areas where different ridge mechanisms are occurring on the MAR. In addition, a specific classification for similar sized events would also aid the swarm classification system through removing any mainshock-aftershock sequences. However, there are limited events of this nature in this current dataset (Figure 11).

5.6 Overall usefulness of using a global dataset for swarm analysis

The usefulness of this work is highlighted by the volume of potential swarms (150+) found using this simple cluster method. In searching the academic literature on swarms on this portion of the

Mid-Atlantic Ridge we only identify 40 swarms over 70 years from 5 published papers (Bergman and Solomon, 1990; Crane et al., 1997; Goslin et al., 2005; Klein, 1976; Cesca et al., 2023). Here in this cluster study of a generic global database in the past 25 years, we have identified 170+ swarms (Table 2) as compared to the five swarm events in published literature (Table 3). Although we are not able to obtain the exact number of the events as compared to the limited amount of published data, we are still able to add to the knowledge of the tectonic behavior of the largest divergent boundary on our planet.

Notably, we have identified a potential 170+ swarms not discussed in the current literature, as well as confirming anomalous activity such as a recent 300+ event from 2022 (Figure 9b; Cesca et al., 2023). Furthermore, the majority of all events would be classified as swarms rather than mainshock-aftershock sequences with similar magnitude (e.g., swarms, Figure 11). The broad analysis here provides potential future studies with a benchmark to exploring spatial and temporal changes on a significant tectonic feature for our planet—a clear use of a global dataset coming from the uniform nature by which the data is collected. As all the data from this dataset is collected in the same way, it is easier to compare events than say trying to compare local high-resolution analysis that varies in data quality and acquisition methodology.

6 Conclusion

In this study, we present a simple cluster analysis using a global dataset to assess what information can be reliably understood about Mid-Atlantic Ridge swarms. We test 400 different combinations of spatial and temporal thresholds (Figure 6) and find that distance between earthquakes has limited variability in producing swarm characteristics and conclude that earthquakes in a cluster occur within 20 km of each other (Figure 7). In addition, the swarms captured in this study most often occur within a day.

In comparing our work to existing swarms within the literature over the past 25 years, the location and timing of some of our swarms appear to be well represented (Table 3). Yet, the use of a global earthquake database is unable to accurately capture earthquakes less than magnitude 3 (Figure 2f) and therefore this method is unable to consistently represent the correct number of earthquakes per swarm event (e.g., Table 3).

Despite the limited ability to capture smaller events, the usefulness of this method is in the volume of swarms that are occurring on the ridge. Fundamentally, the work here adds to the understanding of the largest divergent plate boundary in the world by providing basic seismic attributes for over 170 new swarm events (including timing, location, and frequency of swarms). Given the usefulness of using a global dataset to better understand the seismology of the Mid-Atlantic Ridge, we encourage the application of the method presented here on other tectonic environments.

Data availability statement

The original contributions presented in the study are included in the article/Supplementary Material and in an online

repository (Zhong et al., 2026), further inquiries can be directed to the corresponding author.

Author contributions

RZ: Writing – original draft, Software, Investigation, Funding acquisition, Writing – review and editing, Visualization, Resources, Methodology, Formal Analysis, Validation, Project administration, Conceptualization, Data curation. JR: Formal Analysis, Writing – review and editing, Visualization, Writing – original draft, Validation. PH: Investigation, Visualization, Methodology, Supervision, Writing – review and editing, Conceptualization, Resources, Funding acquisition, Writing – original draft, Project administration, Formal Analysis, Validation.

Funding

The author(s) declared that financial support was received for this work and/or its publication. This research was enabled by support from a Natural Sciences and Engineering Research Council of Canada USRA grant for RZ (USRA-582605-2023) and a Natural Sciences and Engineering Research Council of Canada Discovery Grant for PJH (RGPIN-2022-03084).

Conflict of interest

The author(s) declared that this work was conducted in the absence of any commercial or financial relationships

References

- Bergman, E. A., and Solomon, S. C. (1990). Earthquake swarms on the mid-atlantic ridge: products of magmatism or extensional tectonics? *J. Geophys. Res.* 95 (B4), 4943–4965. doi:10.1029/JB095iB04p04943
- Björnsson, S., Einarsson, P., Tulinius, H., and Hjartardóttir, Á. R. (2020). Seismicity of the Reykjanes peninsula 1971–1976. *J. Volcanol. Geotherm. Res.* 391. doi:10.1016/j.jvolgeores.2018.04.026
- Bohnenstiehl, D. R., Tolstoy, M., Dziak, R. P., Fox, C. G., and Smith, D. K. (2002). Aftershock sequences in the mid-ocean ridge environment: an analysis using hydroacoustic data. *Tectonophysics* 354, 49–70. doi:10.1016/S0040-1951(02)00289-5
- Bohnenstiehl, D. W. R., Tolstoy, M., Smith, D. K., Fox, C. G., and Dziak, R. P. (2003). Time-clustering behavior of spreading-center seismicity between 15 and 35°N on the mid-atlantic ridge: observations from hydroacoustic monitoring. *Phys. Earth Planet. Interiors* 138 (2), 147–161. doi:10.1016/S0031-9201(03)00113-4
- Brocher, T. M. (1983). T-phases from an earthquake swarm on the mid-atlantic ridge at 31.6°N. *Mar. Geophys. Res.* 6, 39–49. doi:10.1007/BF00300397
- Cesca, S., Metz, M., Büyükkakpınar, P., and Dahm, T. (2023). The energetic 2022 seismic unrest related to magma intrusion at the north mid-atlantic ridge. *Geophys. Res. Lett.* 50, e2023GL102782. doi:10.1029/2023GL102782
- Cox, G. M. T. W., Mitchell, R. N., Hasterok, D., and Gard, M. (2018). Linking the rise of atmospheric oxygen to growth in the Continental phosphorus inventory. *Earth Planet. Sci. Lett.* doi:10.1016/j.epsl.2018.02.016
- Crane, K., Johnson, L., Appelgate, B., Nishimura, C., Buck, R., Jones, C., et al. (1997). Volcanic and seismic swarm events on the Reykjanes ridge and their similarities to events on Iceland: results of a rapid response mission. *Mar. Geophys. Res.* 19, 319–338. doi:10.1023/A:1004298425881
- Crawford, W. C., Rai, A., Singh, S. C., Cannat, M., Escartin, J., Wang, H., et al. (2013). Hydrothermal seismicity beneath the summit of lucky strike volcano, mid-atlantic ridge. *Earth Planet. Sci. Lett.* 373, 118–128. doi:10.1016/j.epsl.2013.04.028
- de Melo, G. W. S., Mitchell, N. C., Zahradnik, J., Dias, F., and do Nascimento, A. F. (2021). Oceanic tectonotectonics from regional earthquake recordings: the 4–5°N mid-atlantic ridge. *Tectonophysics* 819. doi:10.1016/j.tecto.2021.229063
- Dziak, R. P., Smith, D. K., Bohnenstiehl, D. W. R., Fox, C. G., Desbruyeres, D., Matsumoto, H., et al. (2004). Evidence of a recent magma dike intrusion at the slow spreading lucky strike segment, mid-atlantic ridge. *J. Geophys. Res. Solid Earth* 109 (12), 1–15. doi:10.1029/2004JB003141
- German, C. R., Bennett, S. A., Connelly, D. P., Evans, A. J., Murton, B. J., Parson, L. M., et al. (2008). Hydrothermal activity on the southern mid-atlantic ridge: tectonically- and volcanically-controlled venting at 4–5°S. *Earth Planet. Sci. Lett.* 273 (3–4), 332–344. doi:10.1016/j.epsl.2008.06.048
- Giusti, M., Perrot, J., Dziak, R. P., Sukhovich, A., and Maia, M. (2018). The August 2010 earthquake swarm at north FAMOUS-FAMOUS segments, mid-atlantic ridge: geophysical evidence of dike intrusion. *Geophys. J. Int.* 215 (1), 181–195. doi:10.1093/gji/ggy239
- Goslin, J., Lourenço, N., Dziak, R. P., Bohnenstiehl, D. R., Haxel, J., and Luis, J. (2005). Long-term seismicity of the Reykjanes ridge (north Atlantic) recorded by a regional hydrophone array. *Geophys. J. Int.* 162 (2), 516–524. doi:10.1111/j.1365-246X.2005.02678.x
- Hasterok, D., Halpin, J., Collins, A., Hand, M., Kreemer, C., Gard, M., et al. (2022). New maps of global geologic provinces and tectonic plates: global tectonics data and QGIS project file (Version 1) [Data set]. *Zenodo*. doi:10.5281/zenodo.6586972->
- Klein, F. W. (1976). Earthquake swarms and the semidiurnal solid Earth tide. *Geophys. J. R. Astronomical Soc.* 45(2), 245–295. doi:10.1111/j.1365-246X.1976.tb00326.x
- Läderach, C., Korger, E. I. M., Schlindwein, V., Müller, C., and Eckstaller, A. (2012). Characteristics of tectonomagmatic earthquake swarms at the southwest Indian Ridge between 16°E and 25°E: tectonomagmatic swarms at the SW Indian ridge. *Geophys. J. Int.* 190 (1), 429–441. doi:10.1111/j.1365-246X.2012.05480.x

that could be construed as a potential conflict of interest.

Generative AI statement

The author(s) declared that generative AI was not used in the creation of this manuscript.

Any alternative text (alt text) provided alongside figures in this article has been generated by Frontiers with the support of artificial intelligence and reasonable efforts have been made to ensure accuracy, including review by the authors wherever possible. If you identify any issues, please contact us.

Publisher's note

All claims expressed in this article are solely those of the authors and do not necessarily represent those of their affiliated organizations, or those of the publisher, the editors and the reviewers. Any product that may be evaluated in this article, or claim that may be made by its manufacturer, is not guaranteed or endorsed by the publisher.

Supplementary material

The Supplementary Material for this article can be found online at: <https://www.frontiersin.org/articles/10.3389/feart.2026.1731117/full#supplementary-material>

- McNutt, S. R. (1996). "Seismic monitoring and eruption forecasting of volcanoes: a review of the state-of-the-art and case histories," in *Monitoring and mitigation of volcanic hazards*. Editors R. Scarpa, and R. Tilling (Berlin, Germany: Springer-Verlag), 3, 99–146.
- Neves, M. C., Bott, M. H. P., and Searle, R. C. (2004). Patterns of stress at midocean ridges and their offsets due to seafloor subsidence. *Tectonophysics* 386 (3–4), 223–242. doi:10.1016/j.tecto.2004.06.010
- Schlaphorst, D., Rychert, C. A., Harmon, N., Hicks, S. P., Bogiatzis, P., Kendall, J.-M., et al. (2023). Local seismicity around the chain transform fault at the mid-atlantic ridge from OBS observations. *Geophys. J. Int.* 234 (2), 1111–1124. doi:10.1093/gji/ggad124
- Schlindwein, V. (2012). Teleseismic earthquake swarms at ultraslow spreading ridges: indicator for dyke intrusions? *Geophys. J. Int.* 190 (1), 442–456. doi:10.1111/j.1365-246X.2012.05502.x
- Smith, D. K., Tolstoy, M., Fox, C. G., Bohnenstiehl, D. R., Matsumoto, H., and Fowler, M. J. (2002). Hydroacoustic monitoring of seismicity at the slow-spreading mid-atlantic ridge. *Geophys. Res. Lett.* 29 (11), 13–14. doi:10.1029/2001GL013912
- U.S. Geological Survey (USGS) (2024a). Earthquake hazards program (EHP). Available online at: <https://earthquake.usgs.gov/earthquakes> (Accessed September 10, 2024).
- U.S. Geological Survey (USGS) (2024b). Earthquake place names. Available online at: <https://earthquake.usgs.gov/data/comcat/#place> (Accessed September 10, 2024).
- Wilson, J. T. (1965). Transform faults, Oceanic ridges, and magnetic anomalies southwest of Vancouver island. *Science* 150, 482–485. doi:10.1126/science.150.3695.482
- Zhong, R., Rich, J., and Heron, P. (2026). Earthquake data and cluster analysis along the mid-atlantic ridge (2000–2024) [Data set]. *Zenodo*. doi:10.5281/zenodo.18432550